Electronic Supplementary Material (ESI) for ChemComm.

Supporting information

Screening of the glycopolymer library for GM1 mimetics by the "carbohydrate module method"

Masanori Nagao*, Takeshi Uemura, Tasuku Horiuchi, Yu Hoshino and Yoshiko Miura*

Department of Chemical Engineering, Kyushu University, 744 Motooka, Nishi-ku, Fukuoka 819-0395, Japan.

E-mail: miuray@chem-eng.kyushu-u.ac.jp

Materials

The following chemical agents were purchased from commercial sources, and were used as received: Deutrium oxide (D_2O), pottasium hydroxide (KOH), ascorbic acid, and sodium ascorbate ($_L$-Asc-Na) were purchased from Kanto Chemical (Tokyo, Japan). Acrylamide, copper(II) sulfate pentahydrate ($CuSO_4$), Eosin Y, and hydrochloric acid (HCl) were purchased from Wako Pure Chemical Industries (Osaka, Japan). Sigmacote®,cholera toxin B subunit (CTB) and monosialoganglioside GM1 from bovine brain was purchased from Sigma Aldrich (St. Louis, USA). Acrylamide (AAm) were purified by recrystallization from MeOH. 3-Butynyl acrylamide (BtnAAm),[1] galactose azide,[2] Neu5Ac azide,[2] tris(benzyltriazolyl-methyl)amine (TBTA),[3] and a RAFT agent 2-((((3-((2,3-dihydroxypropyl)amino)-3-oxopropyl)thio)carbonothioyl)thio)propanoic acid (DAOCTPA)[4] was synthesized referring the previous reports.

Characterization

Proton and carbon nuclear resonance (^{1}H NMR and ^{13}C NMR) spectra were recorded on a JEOL-ECP400 spectrometer (JEOL, Tokyo, Japan) using D_2O as a deuterated solvent. Size exclusion chromatography (SEC) with water as the solvent was performed on a JASCO DG-980-50 degasser equipped with a JASCO PU-980 pump (JASCO Co., Tokyo, Japan), a Shodex OH pak SB-G guard column, a Shodex OH pak SB-803 HQ column (Showa Denko, Tokyo, Japan) and a JASCO RI-2031 Plus RI detector. SEC analyses were performed at a flow rate of 0.5 mL/min by injecting 20 μL of a polymer solution (1 g/L) in a 100 mM $NaNO_3$ aqueous solution. The SEC system was calibrated using a pullulan standard (Shodex). All the samples for SEC analysis were previously filtered through a 0.45 μm filter. UV-vis spectra were recorded at room temperature using an Agilent 8453 spectrophotometer (Agilent Technologies, Santa Clara, CA, USA). For the analysis of the glycopolymer-immobilized gold surfaces, x-ray photoelectron spectroscopy (XPS) (AXISultra; Shimazu/Kratos, Kyoto, Japan) measurement was performed. All SPRI measurements were performed using MultiSPRinter (Toyobo Co., Ltd., Osaka, Japan). The water used in this research was purified using a Direct-Q Ultrapure Water System (Merck, Ltd, Darmstadt, Germany).

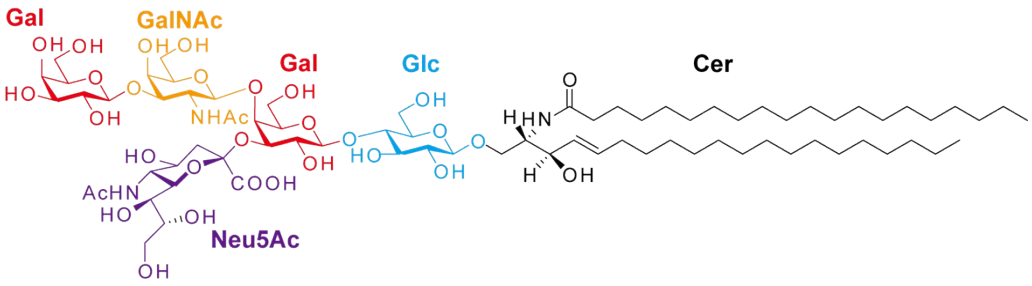

Figure S1. Molecular structure of GM1 ganglioside.

Synthesis of galactose acrylamide (GalAAm)

Acrylamide derivative of galactose (GalAAm) was synthesized by Huisgen reaction. TBTA (265 mg, 0.5 mmol), galactose azide (1.02 g, 5.0 mmol), BtnAAm (615 mg, 5.0 mmol), and $CuSO_4$ (80 mg, 0.5 mmol) were dissolved in MeOH (25 mL) / H_2O (25 mL) mixture. The oxygen was removed by bubbling nitrogen. $_L$-Asc-Na (200 mg, 1.0 mmol) was added and stirred at room temperature overnight under nitrogen. The solution was concentrated under reduced pressure, and the precipitate was filtered. The crude product was purified by reverse-phase chromatography (Biotage SNAP ULTRA C18, gradient from water to methanol). The fraction containing the product was concentrated under reduced pressure and stirred with a metal scavenger (1.0 g) at room temperature overnight. After removal of metal scavenger of SiliaMets by filtration, the solution was concentrated under reduced pressure and galactose acrylamide (GalAAm) product was obtained by freeze-drying (714 mg, 44%).

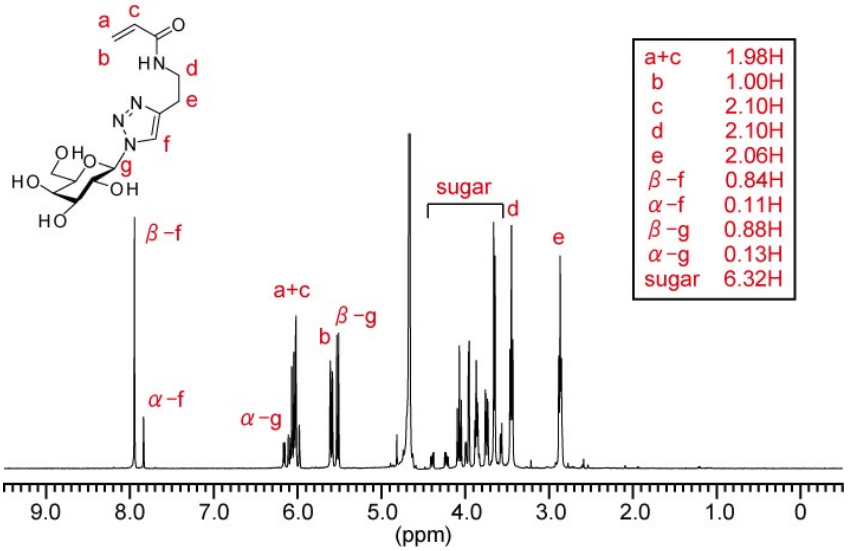

Figure S2-1. ^{1}H NMR spectrum of GalAAm (400 MHz, D_2O).

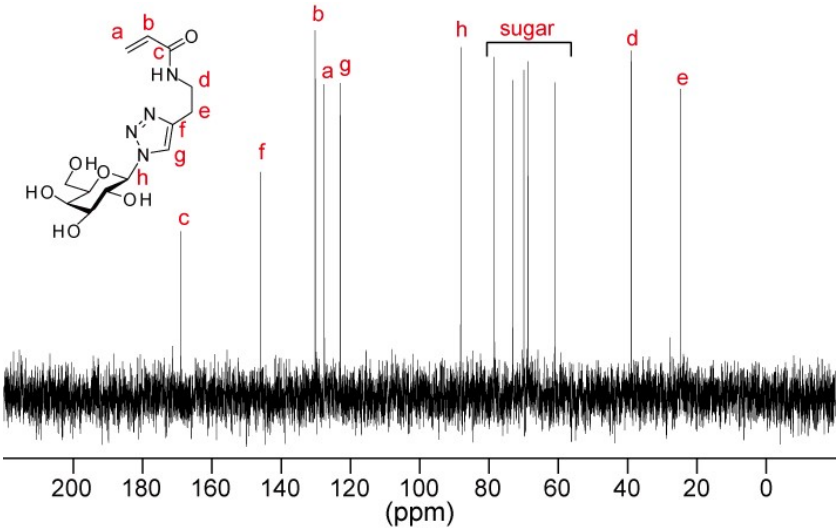

Figure S2-2. ^{13}C NMR spectrum of GalAAm (400 MHz, D_2O).

Synthesis of Neu5Ac acrylamide (Neu5AcAAm)

Acrylamide derivative of neuraminic acid (Neu5AcAAm) was synthesized by Huisgen reaction. TBTA (53 mg, 0.1 mmol), Neu5Ac azide (358 mg, 1.0 mmol), BtnAAm (135 mg, 1.1 mmol), and $CuSO_4$ (16 mg, 0.10 mmol) were dissolved in MeOH (5 mL) / H_2O (5 mL) mixture. The oxygen was removed by bubbling nitrogen. $_L$-Asc-Na (40 mg, 0.20 mmol) was added and stirred at room temperature overnight under nitrogen. The solution was concentrated under reduced pressure, and the precipitate was filtered. The crude product was purified by the same procedure as GalAAm (195 mg, 41 %).

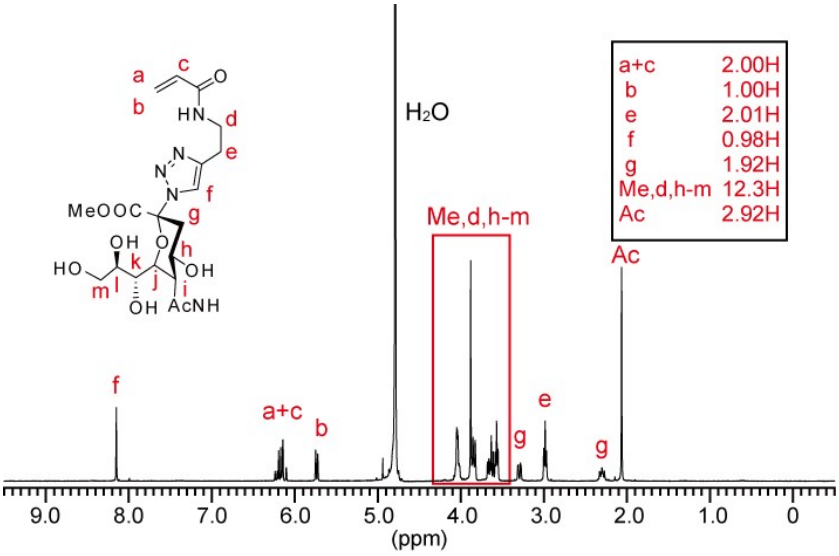

Figure S2-3. ^{1}H NMR spectrum of Neu5AcAAm (400 MHz, D_2O).

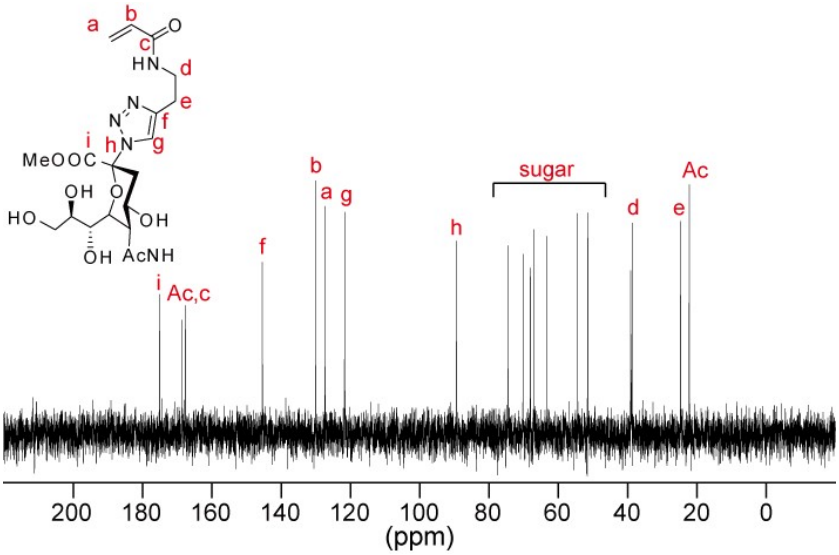

Figure S2-4. ^{13}C NMR spectrum of Neu5AcAAm (400 MHz, D_2O).

General procedure for PET-RAFT polymerization and reduction of trithiocarbonate terminal. Three types of monomers (AAm, GalAAm, and Neu5AcAAm) were polymerized using PET-RAFT polymerization with reference to previous studies.[5] Setting the monomer concentration to 0.5 M, the monomers, RAFT agent (DAOCTPA), photooxidation-reduction catalyst (eosin Y), and reducing agent (ascorbic acid) were dissolved in Milli-Q water (200 μL) at the molar ratio of 100: 1: 0.01: 1. The mixture was put in a well of 96 well plate. The mixture was irradiated by LED lights (λ = 527 nm) at room temperature for 7 h. The conversion rate was determined by ^{1}H NMR, and relative molecular weight and dispersity (M_w/M_n) were calculated by GPC analysis.

Aqueous solution of potassium hydroxide (1 M, 30 μL) was added to each well (200 μL of polymer solution), and the mixture was incubated for 12 h at room temperature. The solution was neutralized with 1 M HCl solution. Then, the polymer solution was added to an ultrafiltration filter (MWCO: 3000), and purification was repeated 3 times in a centrifuge (14000 × g, 15 min). The filter tip was turned over and the sample was collected again in a centrifuge (1000 × g, 10 min) and then freeze-dried to obtain a solid glycopolymer sample.

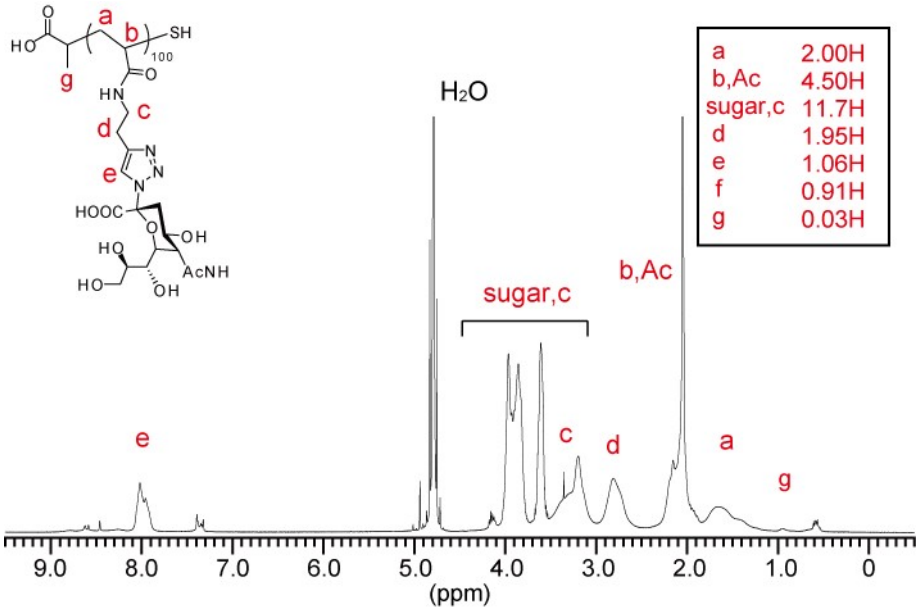

Figure S2-5. ^{1}H NMR spectrum of **G0N100** (400 MHz, D_2O).

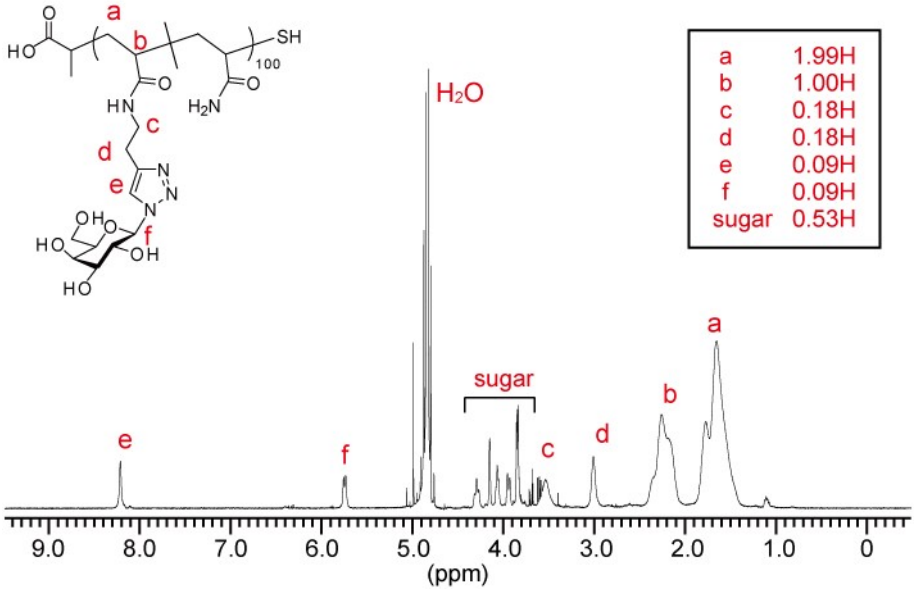

Figure S2-6. ^{1}H NMR spectrum of **G10N0** (400 MHz, D_2O).

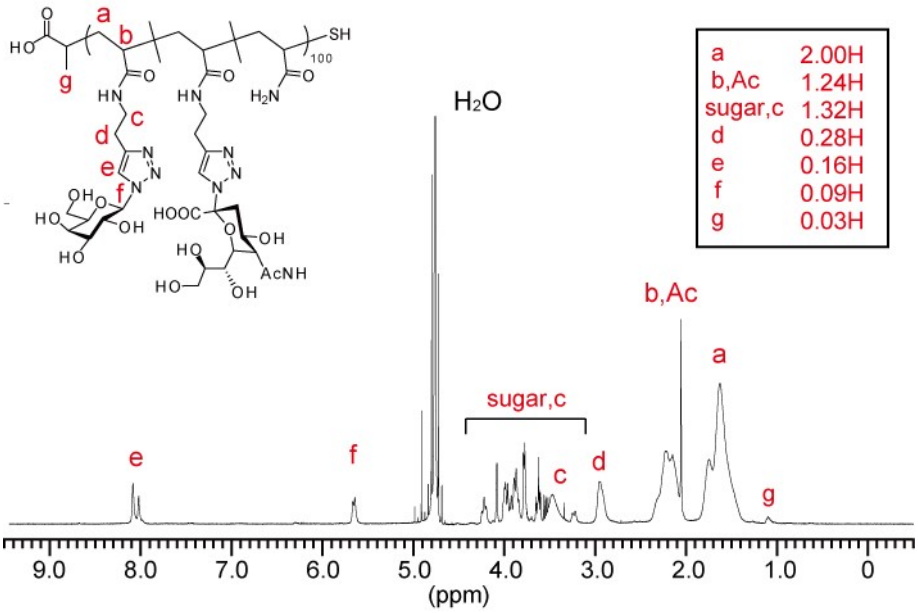

Figure S2-7. ^{1}H NMR spectrum of **G10N10** (400 MHz, D_2O).

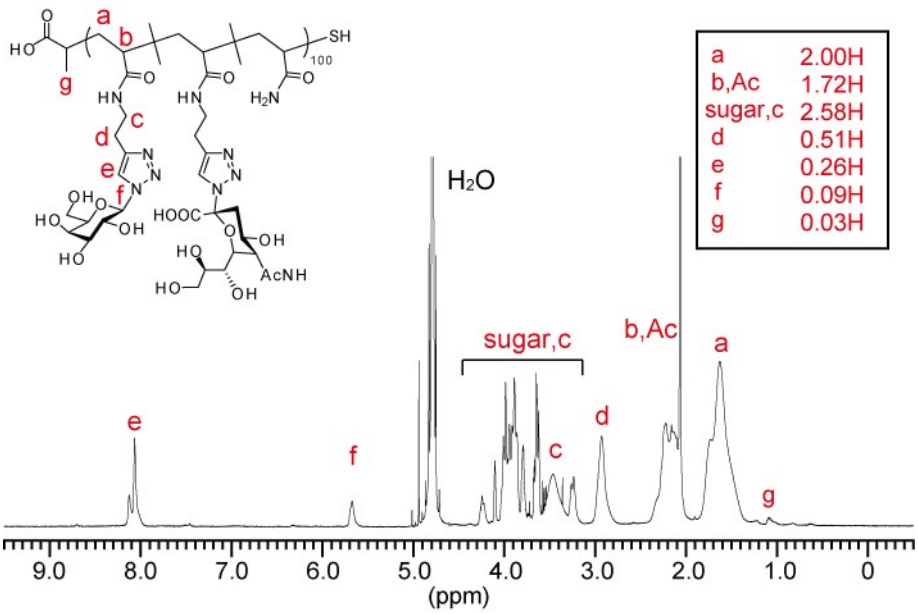

Figure S2-8. ^{1}H NMR spectrum of **G10N20** (400 MHz, D_2O).

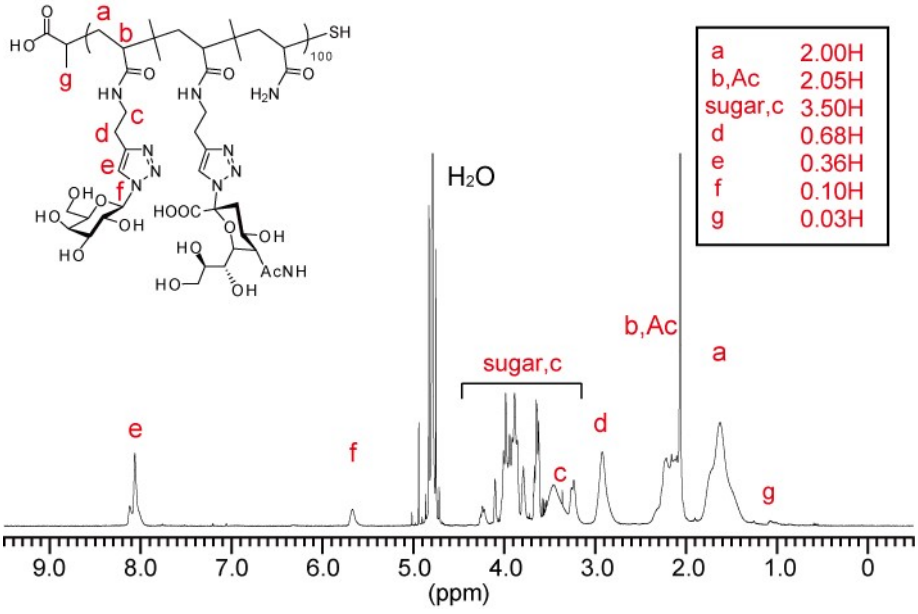

Figure S2-9. ^{1}H NMR spectrum of **G10N30** (400 MHz, D_2O).

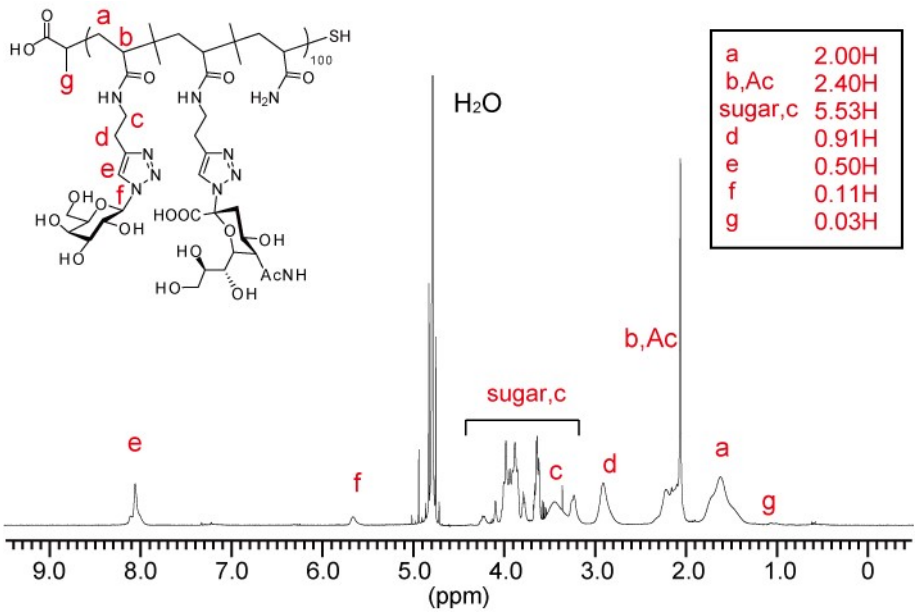

Figure S2-10. ^{1}H NMR spectrum of **G10N40** (400 MHz, D_2O).

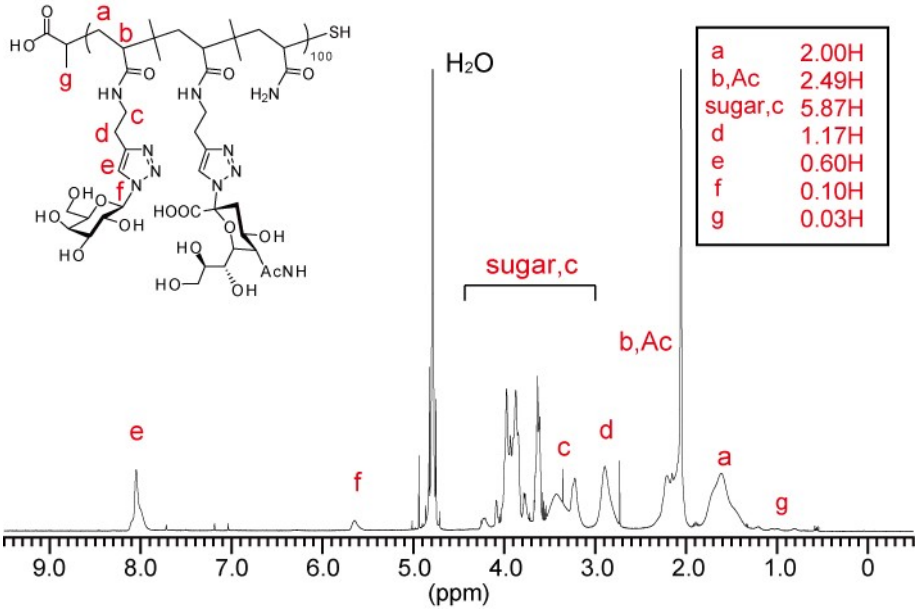

Figure S2-11. ^{1}H NMR spectrum of **G10N50** (400 MHz, D_2O).

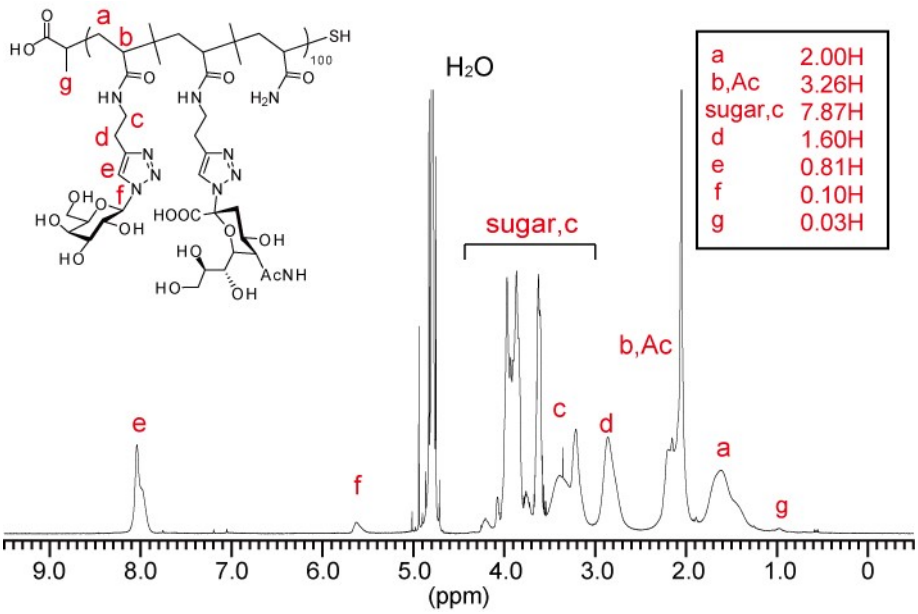

Figure S2-12. ^{1}H NMR spectrum of **G10N70** (400 MHz, D_2O).

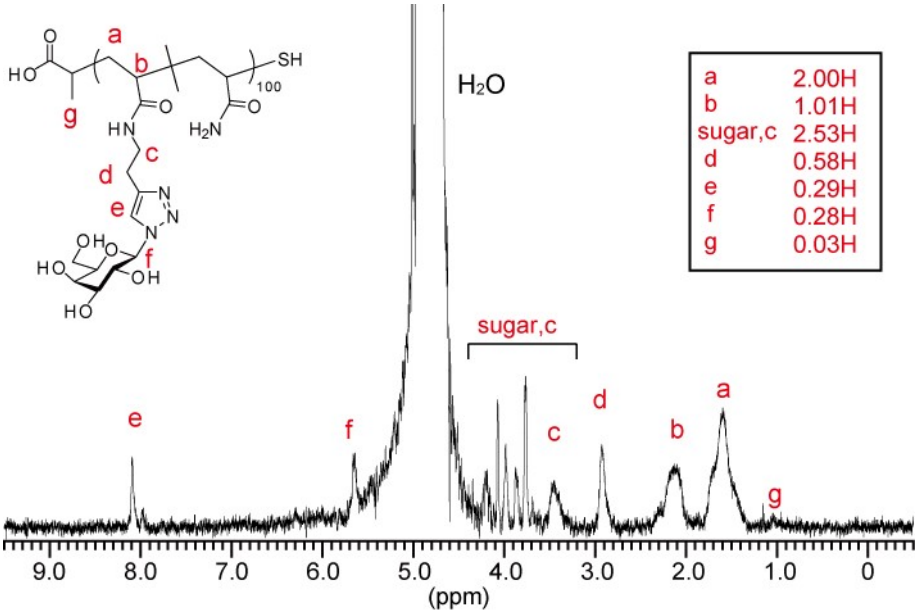

Figure S2-13. ^{1}H NMR spectrum of **G30N0** (400 MHz, D_2O).

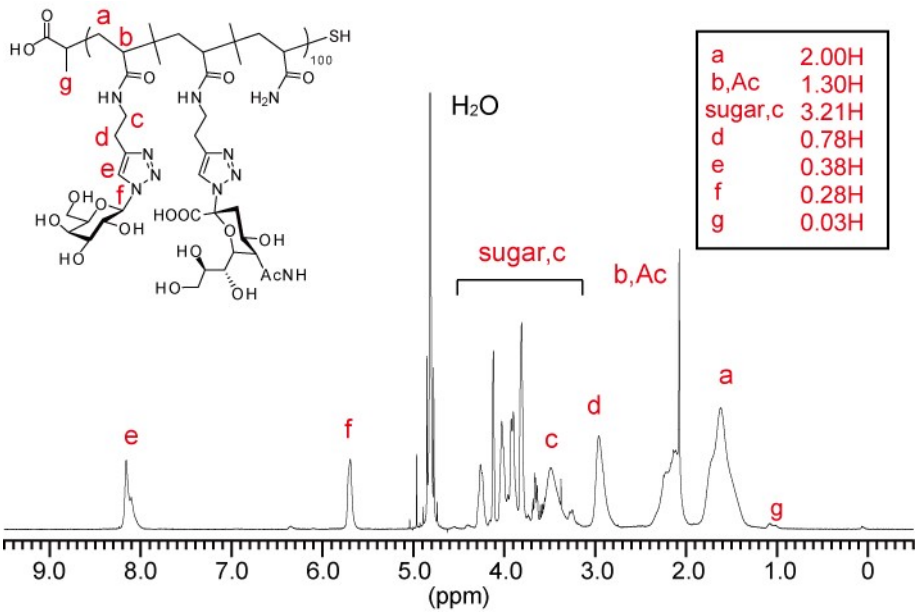

Figure S2-14. ^{1}H NMR spectrum of **G30N10** (400 MHz, D_2O).

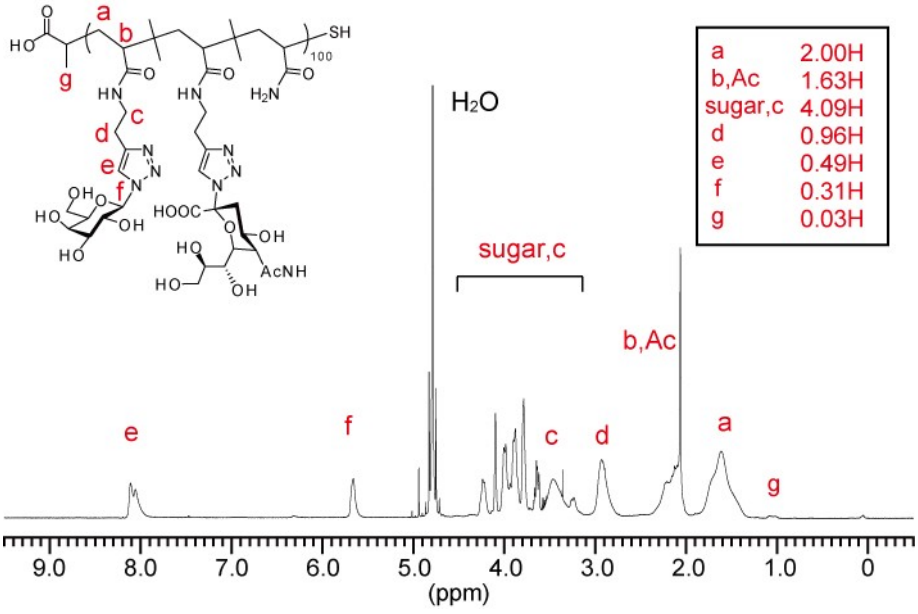

Figure S2-15. ^{1}H NMR spectrum of **G30N20** (400 MHz, D_2O).

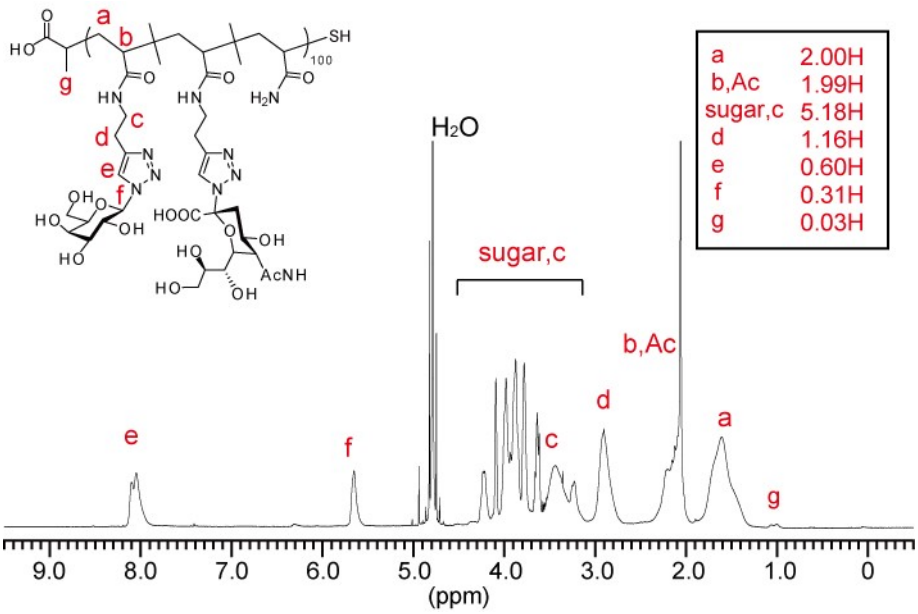

Figure S2-16. ^{1}H NMR spectrum of **G30N30** (400 MHz, D_2O).

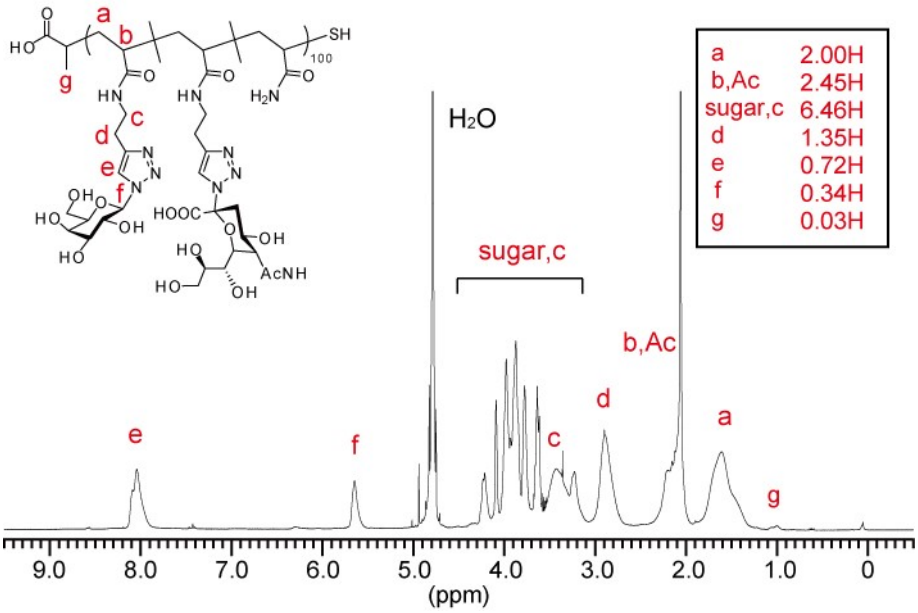

Figure S2-17. ^{1}H NMR spectrum of **G30N40** (400 MHz, D_2O).

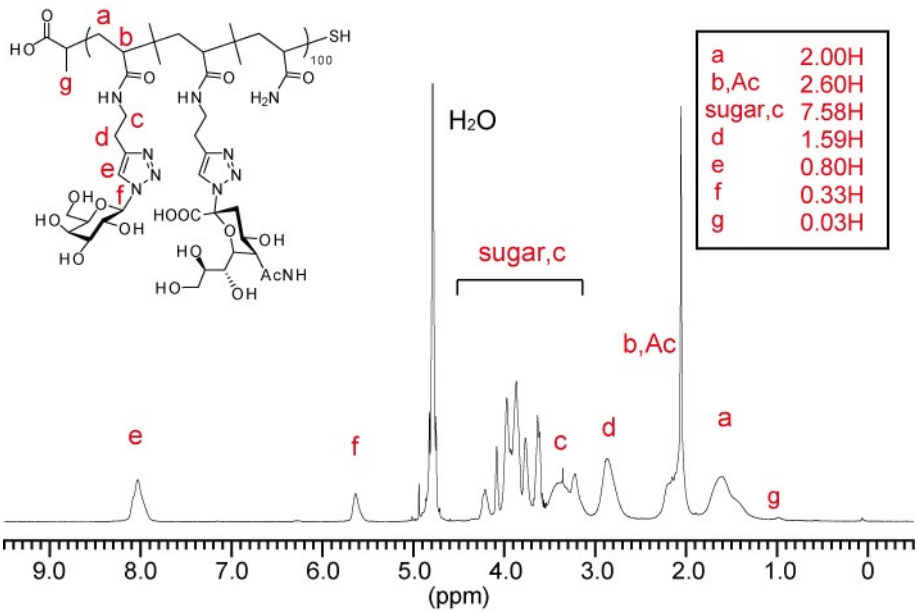

Figure S2-18. ^{1}H NMR spectrum of **G30N50** (400 MHz, D_2O).

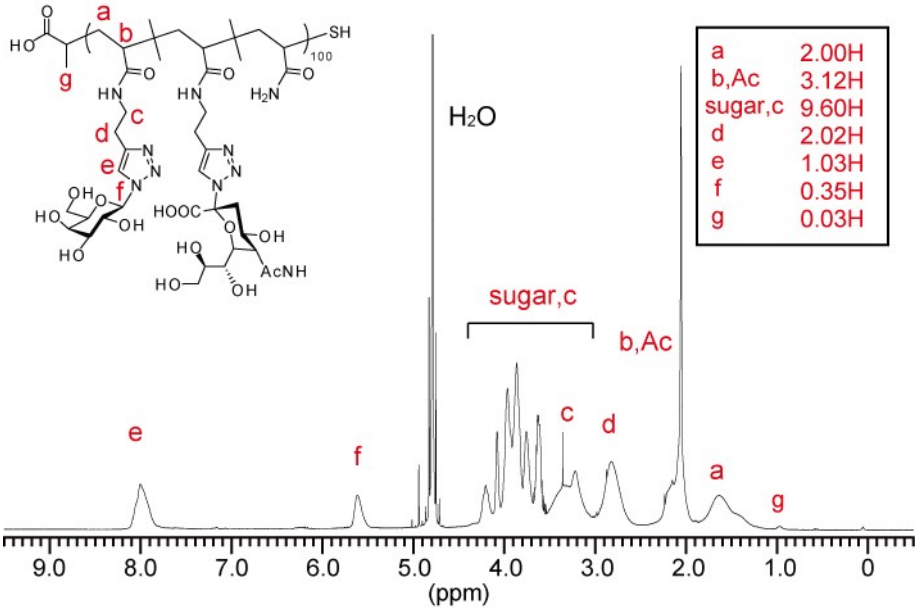

Figure S2-19. ^{1}H NMR spectrum of **G30N70** (400 MHz, D_2O).

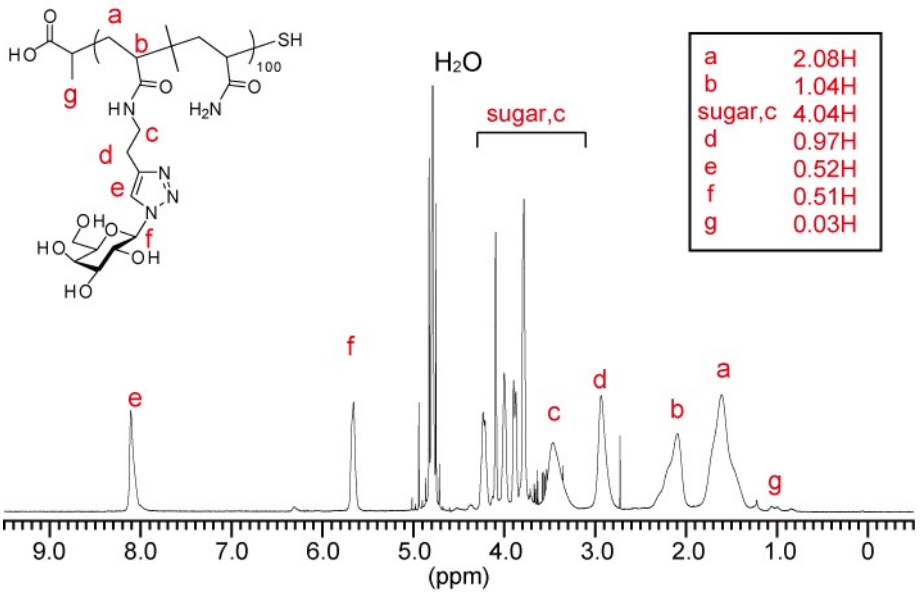

Figure S2-20. ^{1}H NMR spectrum of **G50N0** (400 MHz, D_2O).

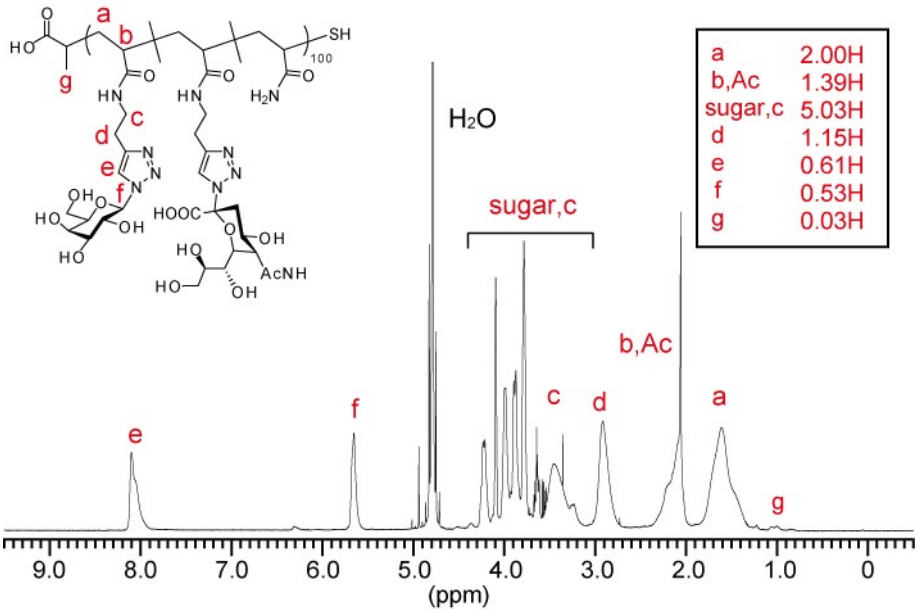

Figure S2-21. ^{1}H NMR spectrum of **G50N10** (400 MHz, D_2O).

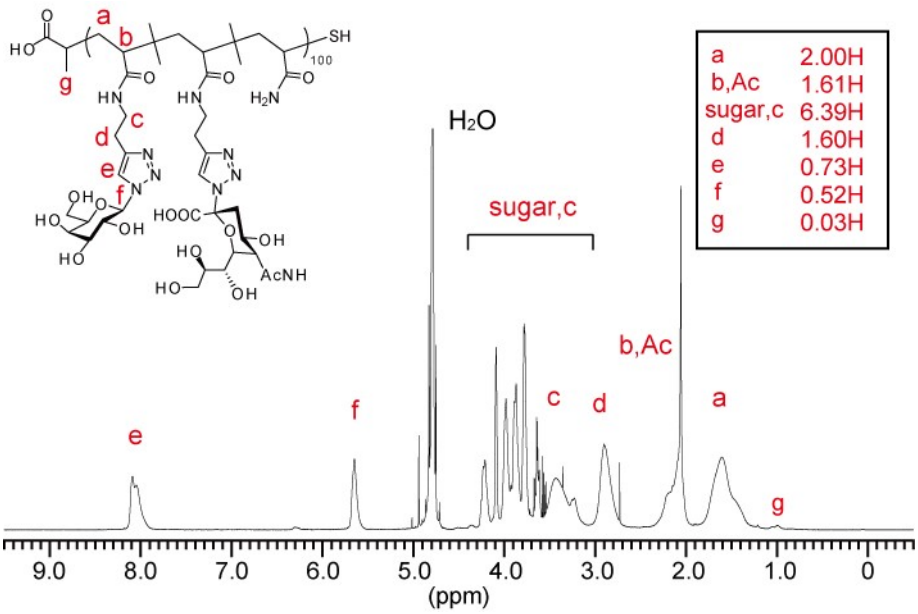

Figure S2-22. ^{1}H NMR spectrum of **G50N20** (400 MHz, D_2O).

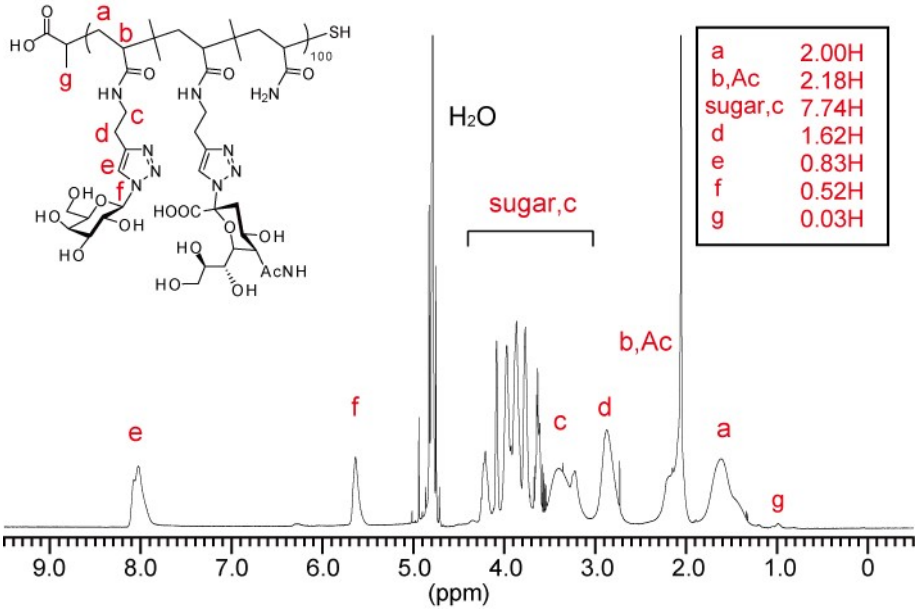

Figure S2-23. ^{1}H NMR spectrum of **G50N30** (400 MHz, D_2O).

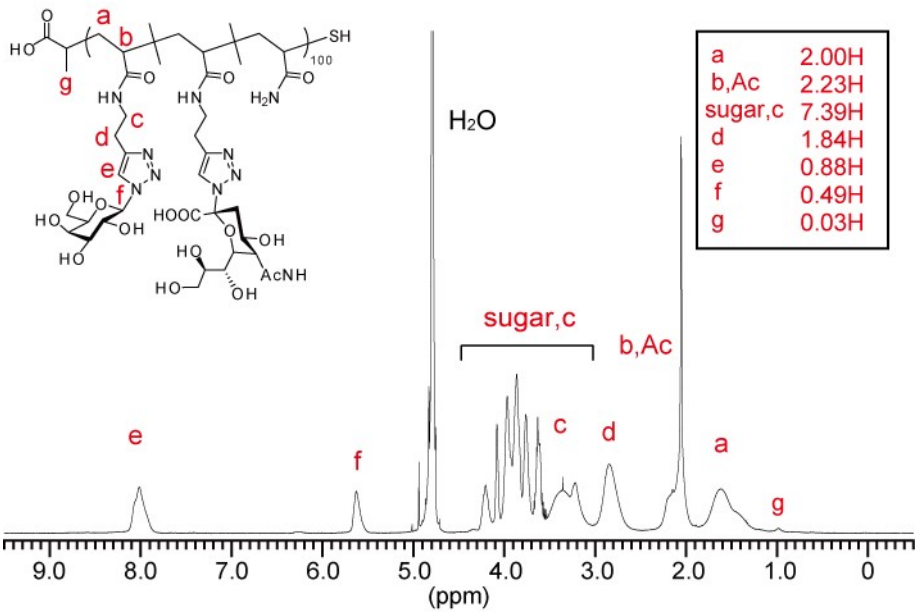

Figure S2-24. ^{1}H NMR spectrum of **G50N40** (400 MHz, D_2O).

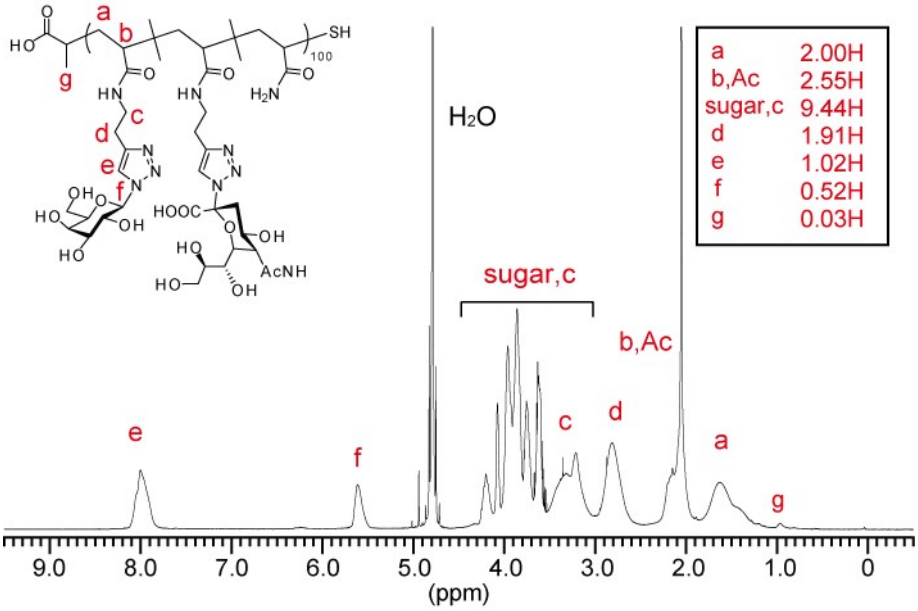

Figure S2-25. ^{1}H NMR spectrum of **G50N50** (400 MHz, D_2O).

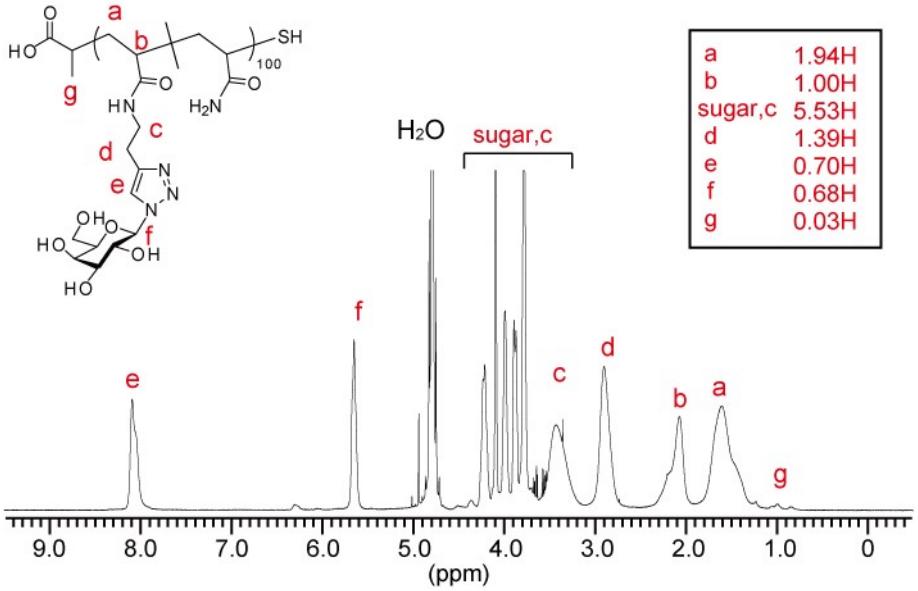

Figure S2-26. ^{1}H NMR spectrum of **G70N0** (400 MHz, D_2O).

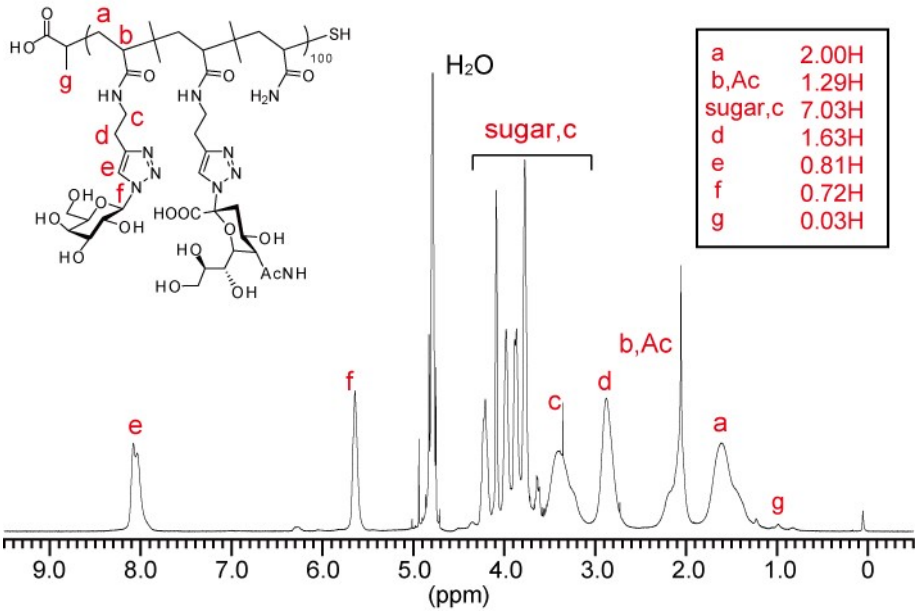

Figure S2-27. ^{1}H NMR spectrum of **G70N10** (400 MHz, D_2O).

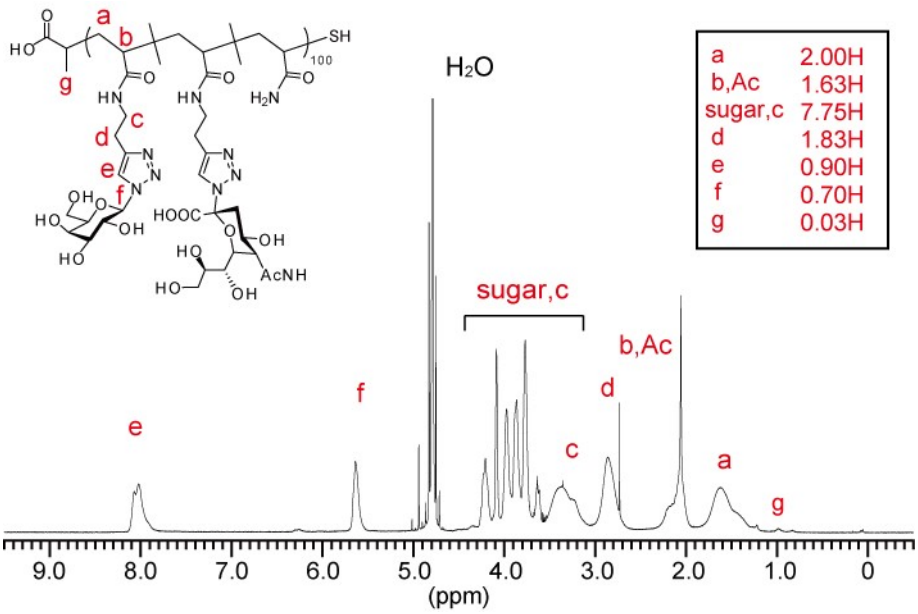

Figure S2-28. ^{1}H NMR spectrum of **G70N20** (400 MHz, D_2O).

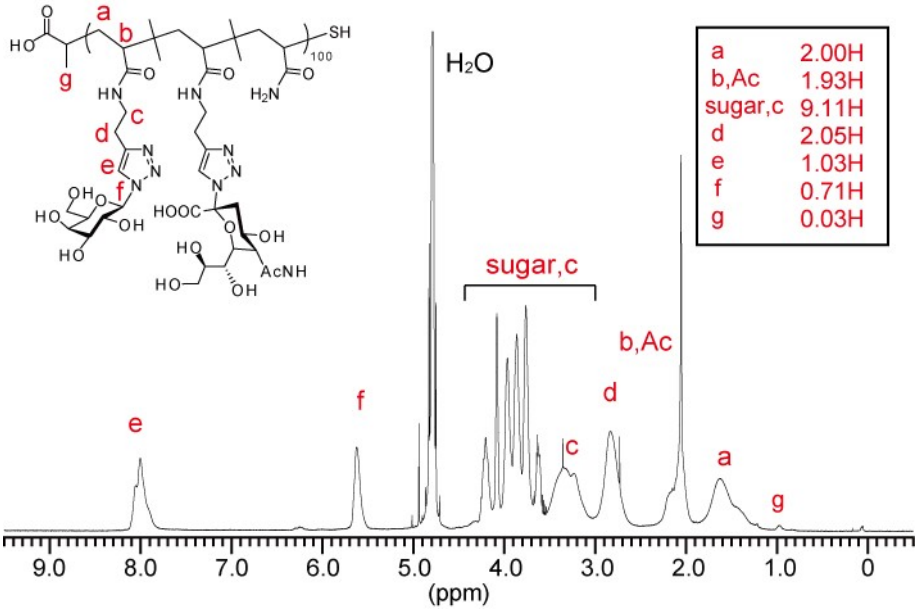

Figure S2-29. ^{1}H NMR spectrum of **G70N30** (400 MHz, D_2O).

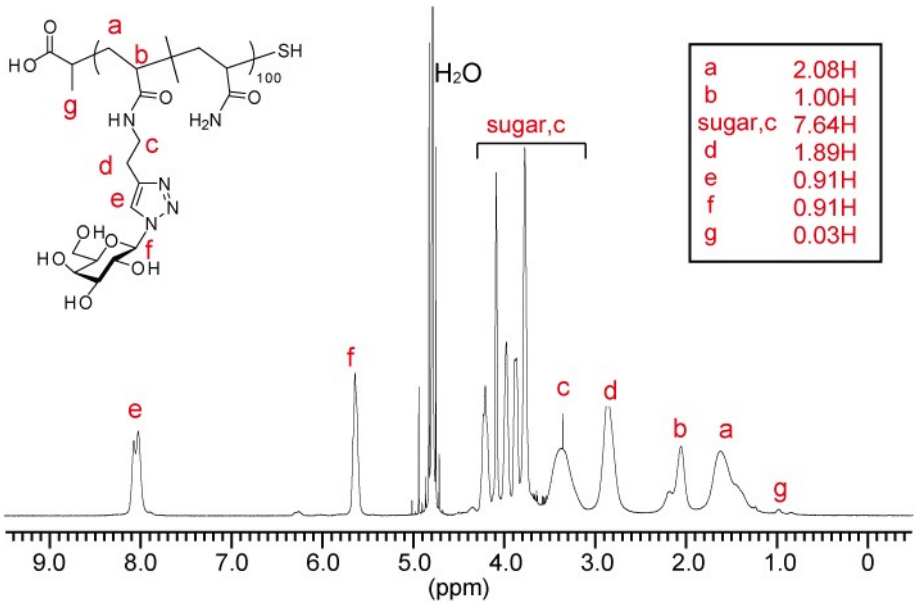

Figure S2-30. ^{1}H NMR spectrum of **G90N0** (400 MHz, D_2O).

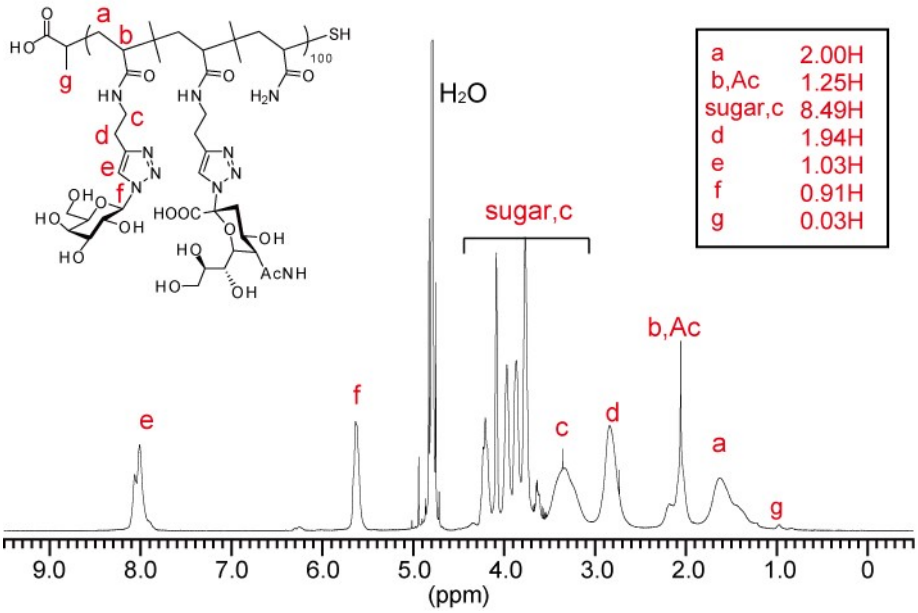

Figure S2-31. ^{1}H NMR spectrum of **G90N10** (400 MHz, D_2O).

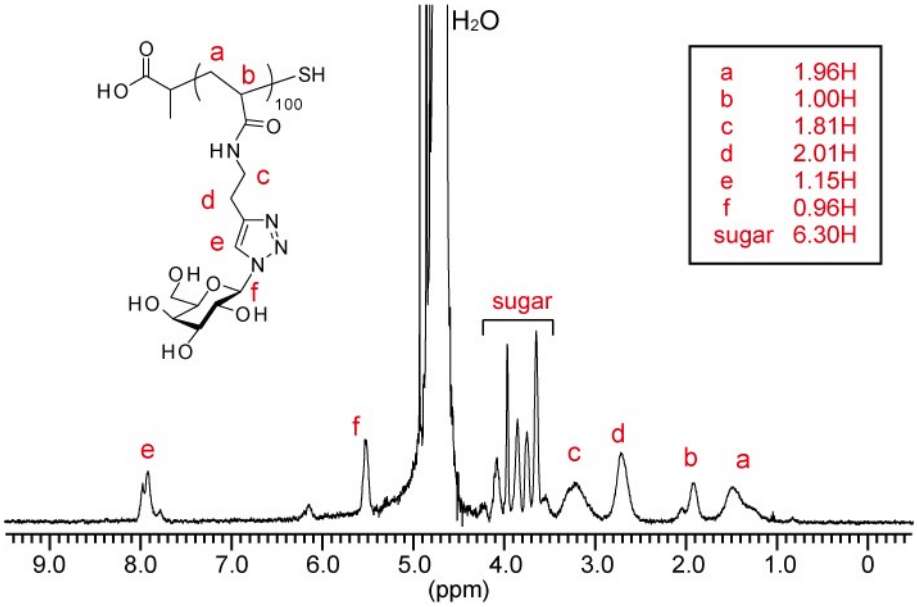

Figure S2-32. ^{1}H NMR spectrum of **G100N0** (400 MHz, D_2O).

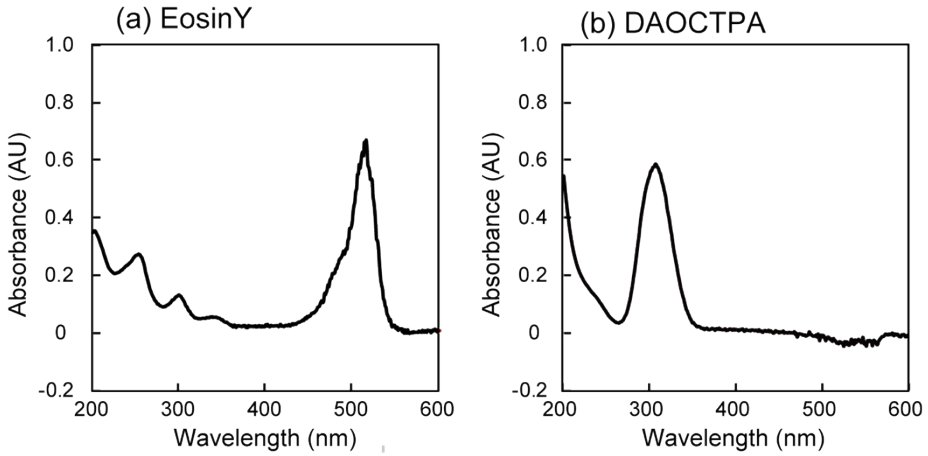

Figure S3. UV-vis absorbance spectra of Eosin Y (a) and DAOCTPA (b). The solvent was water.

Calculation of monomer reactivities from the Mayo−Lewis equation.

The reactivity of each monomer was measured by the Mayo-Lewis equation (Eq.1). Two of the three types of monomers (GalAAm, Neu5AcAAm, and AAm) were polymerized in different monomer ratio. The feed ratio of the two monomers was varied from 20 to 80%. The monomer concentration was 0.5 M, and the monomer, DAOCTPA, eosin Y, and ascorbic acid were dissolved in Milli-Q water (200 μL) at a ratio of 100: 1: 0.01: 1. The polymerization reaction started by irradiation of green light (λ = 527 nm) and was quenched after 30 min by stopping the irradiation. The monomer composition in the obtained polymers was determined by ^{1}H NMR (D_2O) measurement, and the reactivity ratio (r_1, r_2) was calculated by the Mayo-Lewis equation.

$$\frac{d[M_1]}{d[M_2]} = \frac{[M_1]}{[M_2]}\left(\frac{r_1[M_1] + [M_2]}{[M_1] + r_2[M_2]}\right)$$

$$F = \frac{[M_1]}{[M_2]}, f = \frac{d[M_2]}{d[M_1]}$$

$$f = \frac{F(r_1F + 1)}{F + r_2}$$

$$\frac{F(f-1)}{f} = \frac{F^2}{f}r_1 - r_2$$

Eq.1. Mayo-Lewis equation

Table S1. Monomer conversion rates of glycopolymers at each monomer composition after 30 minutes.

	Gal (%)	Neu5Ac (%)	AAm (%)	Conv. (%)
G20A80	20	0	80	5
G40A60	40	0	60	17
G60A40	60	0	40	22
G80A20	80	0	20	28
G80N20	80	20	0	14
G60N40	60	40	0	13
G40N60	40	60	0	14
G20N80	20	80	0	15
N20A80	0	20	80	10
N40A60	0	40	60	9
N60A40	0	60	40	8
N80A20	0	80	20	9

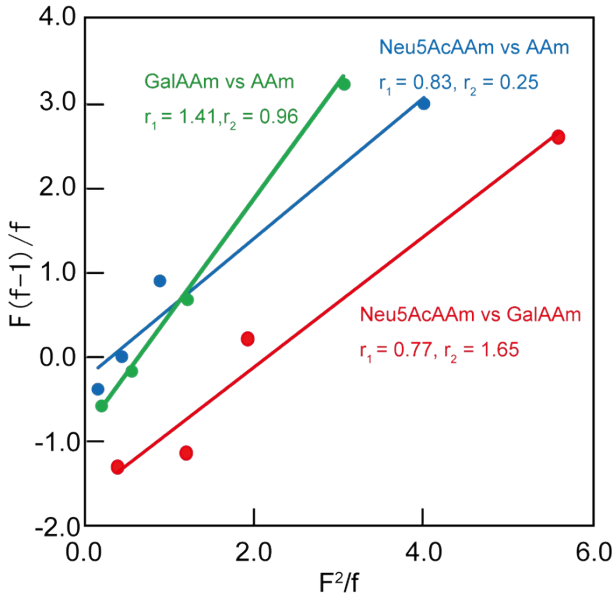

Figure S4. Plot using Mayo-Lewis equation and reactivity ratio of three types of monomers.

UV-vis measurement of the glycopolymers in aqueous solution.

The absorption wavelength of the glycopolymer solution (**G50N20**, 0.015 g/L) before and after the KOH treatment was measured to confirm the removal of trithiocarbonate (λ = 310 nm).

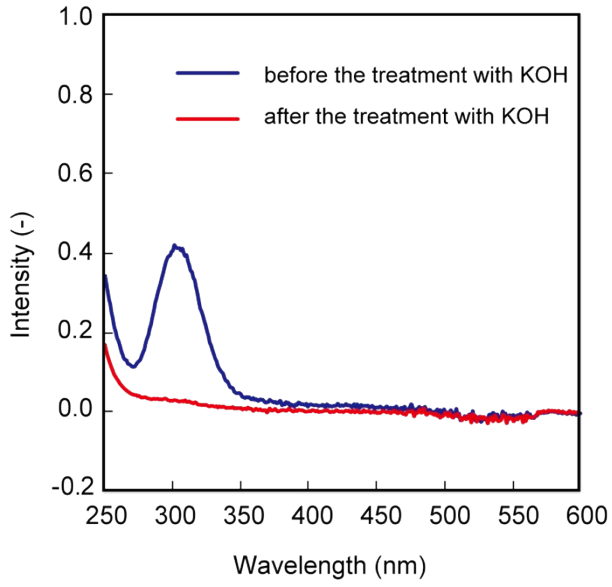

Figure S5. UV-vis absorbance spectra of the glycopolymer **G50N0** before (blue line) and after (red line) the treatment with KOH.

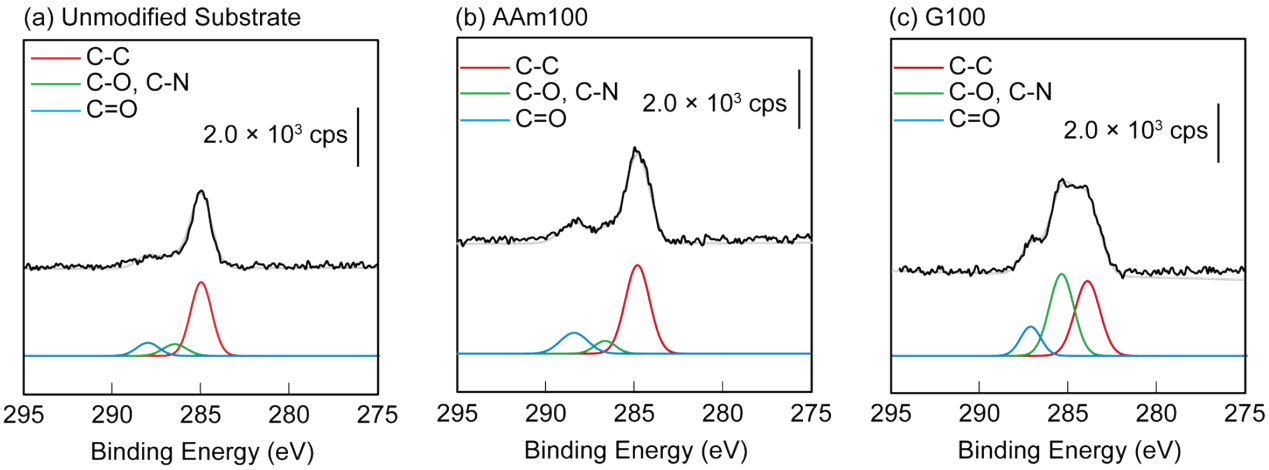

Figure S6. XPS C(1s) spectrum of a) unmodified substrate, b) AAm100 immobilized-gold surface, c) G100 immobilized-gold surface.

General Procedure of SPRI Measurement

SPRI gold chips were prepared by deposition of Cr (1.0 nm) and Au (50 nm) onto S-TIM35 glass substrate. SPRI gold chip was rinsed with EtOH and MilliQ, then dried by air blow. Glycopolymers were immobilized onto the gold spots by incubation of 10 g/L glycopolymer aqueous solution for over 3 h. Prior to the protein adsorption measurement, 10 mM Phosphate buffered saline (PBS) (pH 7.4, 137 mm NaCl, 2.68 mm KCl) was flew through (0.1 mL/min), and SPRI reflectivity change (defined as "SPRI signal") was monitored until the SPRI signal was stable. Then, protein solution with a certain concentration was injected with flow rate of 0.1 mL/min in all experiments, and the SPRI signal was monitored. In the measurement, the SPRI signal was regarded as the amount of protein adsorption. The binding constants of CTB were calculated with the Langmuir isotherm using the SPRI signals

$$\Delta R = \frac{K_a\, c\, \Delta R_{max}}{1 + K_a\, c} \qquad (1)$$

ΔR, ΔR_{max}, c, and K_a are the SPRI signal, the maximum SPRI signal, the protein concentration, and the binding constant, respectively. Based on eq 1, the plots of the SPRI signals were analyzed by nonlinear regression to derive the binding constants.

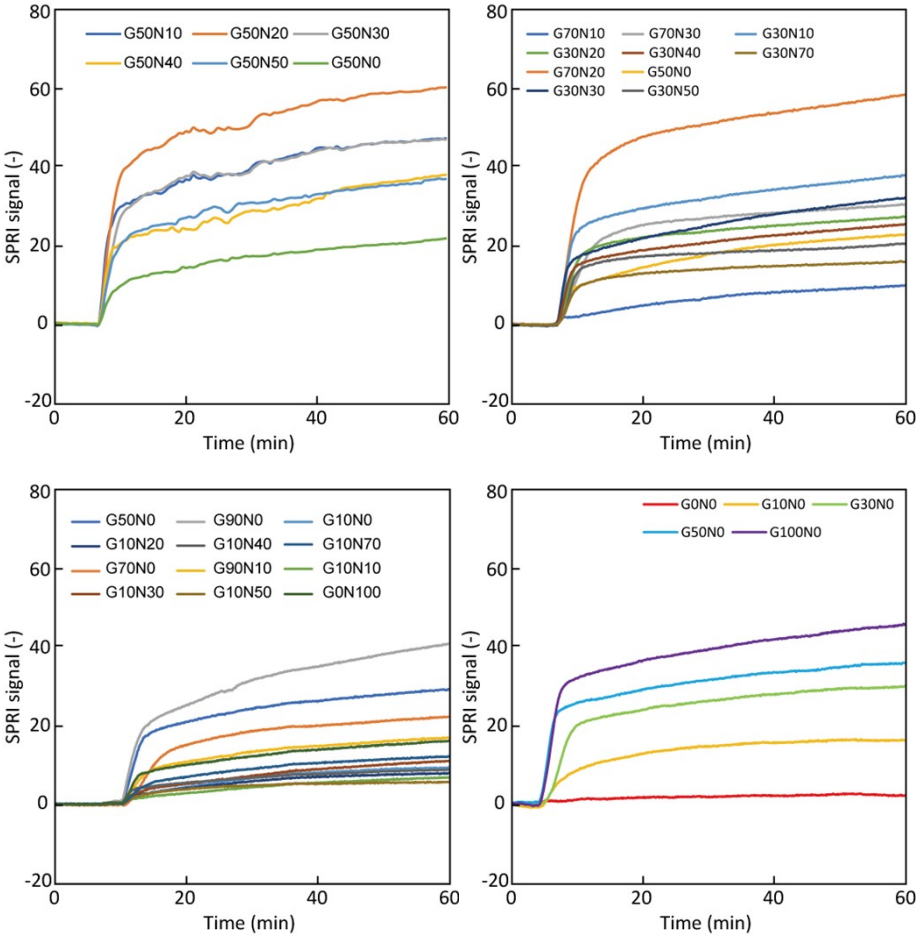

Figure S7. SPRI signal change by addition of CTB (500 nM) to glycopolymers.

SPRI Inhibition Measurement

To confirm that the glycopolymer bound to CTB at the GM1 binding pocket, inhibition measurement was performed. CTB (500 nM) and GM1 (10 μM) were mixed in PBS and equilibrated for over 1 h, and the SPRI signal change by addition of CTB-GM1 pre-equilibrated solution to the glycopolymers was measured over 1 h. Then SPRI signal changes 1 h after addition of the solution was summarized.

Reference

(1) M. Nagao, Y. Kurebayashi, H. Seto, T. Takahashi, T. Suzuki, Y. Hoshino and Y. Miura, *Polym Chem.*, 2016, **7**, 5920–5924.

(2) Y. Tearada, Y. Hoshino and Y. Miura, *Chem. Asian J.*, 2019, **14**, 1021–1027.

(3) C. J. Brassard, X. Zhang, C. R. Brewer, P. Liu, R. J. Clark and L. Zhu, *J. Org. Chem.*, 2016, **81**, 12091−12105.

(4) M. Nagao, Y. Hoshino and Y. Miura, *J. Polm. Sci., Part A: Polym. Chem.*, 2019, **57**, 857−861.

(5) J. Yeow, R. Chapman, J. Xu and C. Boyer, *Polym. Chem.*, 2017, **8**, 5012–5022.